

PORT DOCUMENTATION PAGE

DTIC FILE COPY 2

AD-A224 690 2-1990

2b. DECLASSIFICATION/DOWNGRADING SCHEDULE

4. PERFORMING ORGANIZATION REPORT NUMBER(S)

Technical Report #13

6a. NAME OF PERFORMING ORGANIZATION

SUNY/Buffalo

6b. OFFICE SYMBOL
(If applicable)

1b. RESTRICTIVE MARKINGS

3. DISTRIBUTION/AVAILABILITY OF REPORT

Approved for public release;
distribution unlimited

5. MONITORING ORGANIZATION REPORT NUMBER(S)

7a. NAME OF MONITORING ORGANIZATION

Office of Naval Research

6c. ADDRESS (City, State, and ZIP Code)

Dept. of Chemistry, Acheson Hall,
SUNY/Buffalo, Buffalo, NY 14214

7b. ADDRESS (City, State, and ZIP Code)

Chemistry Program
800 N. Quincy St., Arlington, VA
222178a. NAME OF FUNDING/SPONSORING
ORGANIZATION

Office of Naval Research

8b. OFFICE SYMBOL
(If applicable)

9. PROCUREMENT INSTRUMENT IDENTIFICATION NUMBER

#N00014-88-K-0483

8c. ADDRESS (City, State, and ZIP Code)

Chemistry Program, 800 N. Quincy St.,
Arlington, VA 22217

10. SOURCE OF FUNDING NUMBERS

PROGRAM
ELEMENT NO.PROJECT
NO.TASK
NO.WORK UNIT
ACCESSION NO.

11. TITLE (Include Security Classification)

UNUSUAL PHOTOFRAGMENTATION DYNAMICS IN THE MULTIPHOTON IONIZATION OF
 $\text{Cr}(\text{CO})_6$ /METHANOL VAN DER WAALS HETEROCLUSTERS

12. PERSONAL AUTHOR(S)

William R. Peifer and James F. Garvey

13a. TYPE OF REPORT

Technical

13b. TIME COVERED

FROM TO

14. DATE OF REPORT (Year, Month, Day)

15. PAGE COUNT

43

16. SUPPLEMENTARY NOTATION

Journal of Chemical Physics

17. COSATI CODES

FIELD

GROUP

SUB-GROUP

18. SUBJECT TERMS (Continue on reverse if necessary and identify by block number)

19. ABSTRACT (Continue on reverse if necessary and identify by block number)

Mixed van der Waals clusters containing $\text{Cr}(\text{CO})_6$ and methanol are generated in the free-jet expansion of a pulsed beam of seeded helium and subjected to 248-nm multiphoton ionization (MPI), and the product ions are analyzed by time-of-flight mass spectrometry. We find that the multiphoton dissociation and ionization dynamics of solvated $\text{Cr}(\text{CO})_6$ are strikingly different from those of the naked molecule. Two principle sequences of heterocluster ions are identified in the mass spectrum: a minor sequence with the empirical formula, $\text{S}_n\text{Cr}(\text{CO})_x^+$ ($x=5,6$), where S is a methanol molecule, and a major sequence with the empirical formula, $\text{S}_n\text{Cr}(\text{CO})_x^+$ ($x=0,1,2$). Photoionization of solvated $\text{Cr}(\text{CO})_6$ is thought to give rise to nascent photoions, $\text{S}_n^+[\text{Cr}(\text{CO})_6^*]$, which may subsequently predissociate to $\text{S}_n^+\text{Cr}(\text{CO})_5^+$ on a timescale comparable to the residence time in the ion source, and accounts for the minor sequence.

20. DISTRIBUTION/AVAILABILITY OF ABSTRACT

☒ UNCLASSIFIED/UNLIMITED ☐ SAME AS RPT. ☐ DTIC USERS

21. ABSTRACT SECURITY CLASSIFICATION

Unclassified

22a. NAME OF RESPONSIBLE INDIVIDUAL

Dr. David L. Nelson/Dr. Mark Ross

22b. TELEPHONE (Include Area Code)

(202) 696-4410

22c. OFFICE SYMBOL

OFFICE OF NAVAL RESEARCH

GRANT N00014-88-K-0493

R & T Code 412m008

Technical Report No. 13

**UNUSUAL PHOTOFRAGMENTATION DYNAMICS IN THE
MULTIPHOTON IONIZATION OF $\text{Cr}(\text{CO})_6$ /METHANOL
VAN DER WAALS HETEROCLUSTERS**

by

William R. Peifer and James F. Garvey*

Prepared for Publication
in
The Journal of Chemical Physics

Acheson Hall
Department of Chemistry
University at Buffalo
The State University of New York at Buffalo
Buffalo, NY
14214

Accession For	
NTIS	CRA&I <input checked="" type="checkbox"/>
DTIC	TAB <input type="checkbox"/>
Unannounced <input type="checkbox"/>	
Justification	
By	
Distribution /	
Availability Codes	
Dist	Avail and/or Special
A-1	



Reproduction in whole or in part is permitted for any purpose of the United States Government

This document has been approved for public release and sale; its distribution is unlimited

submitted to J. Chem. Phys. 6/21/90

**Unusual Photofragmentation Dynamics in the Multiphoton
Ionization of $\text{Cr}(\text{CO})_6$ /Methanol van der Waals
Heteroclusters**

William R. Pelfer and James F. Garvey*

Department of Chemistry

State University of New York at Buffalo

Buffalo, New York 14214

ABSTRACT

Mixed van der Waals clusters containing $\text{Cr}(\text{CO})_6$ and methanol are generated in the free-jet expansion of a pulsed beam of seeded helium and subjected to 248-nm multiphoton ionization (MPI), and the product ions are analyzed by time-of-flight mass spectrometry. We find that the multiphoton dissociation and ionization dynamics of solvated $\text{Cr}(\text{CO})_6$ are *strikingly* different from those of the naked molecule. Two principle sequences of heterocluster ions are identified in the mass spectrum: a minor sequence with the empirical formula, $\text{S}_n\text{Cr}(\text{CO})_x^+$ ($x = 5, 6$), where S is a methanol molecule, and a major sequence with the empirical formula, $\text{S}_n\text{Cr}(\text{CO})_x^+$ ($x = 0, 1, 2$). Photoionization of solvated $\text{Cr}(\text{CO})_6$ is thought to give rise to nascent photoions, $\text{S}_n[\text{Cr}(\text{CO})_6^*]^+$, which may subsequently predissociate to $\text{S}_n\text{Cr}(\text{CO})_5^+$ on a timescale comparable to the residence time in the ion source, and accounts for the minor sequence. The major sequence of cluster ions is thought to arise through initial one-photon dissociation of solvated $\text{Cr}(\text{CO})_6$, followed by two-photon nonresonant ionization of the excited primary photoproduct, $\text{S}_n\text{Cr}(\text{CO})_4^*$, and subsequent predissociation (and/or photodissociation) of the excited nascent photoion, $\text{S}_n[\text{Cr}(\text{CO})_4^*]^+$. Differences between the MPI mass spectra of $\text{Cr}(\text{CO})_6/\text{CH}_3\text{OH}$ clusters and $\text{Cr}(\text{CO})_6/\text{CD}_3\text{OD}$ clusters are attributed to the differing efficiencies of CH_3OH and CD_3OD for relaxation of the excited nascent photoions through intracuster V-V energy transfer. Implications are discussed regarding the general utility of MPI as a probe of the electronic structure and reactivity of coordinatively unsaturated organometallic species formed within van der Waals clusters.

INTRODUCTION

Our understanding of the photochemistry and photophysics of transition metal carbonyls has grown tremendously over the past two decades. The photolysis of stable transition metal carbonyls by pulsed UV lasers affords a convenient route to the preparation of highly reactive, coordinatively unsaturated intermediates. These species are important not only because of their fundamental significance in organometallic chemistry,¹ but also because of their relevance to industrially important catalytic reactions.^{2,3} The reactivity of these coordinatively unsaturated species, however, makes their detection and spectroscopic characterization rather difficult. In order to overcome such difficulties, several elegant approaches have been utilized by various groups to detect and characterize the primary products of the UV photolysis of transition metal carbonyls. Yardley and co-workers were able to identify the primary photoproducts of $\text{Fe}(\text{CO})_5$ and $\text{Cr}(\text{CO})_6$ from chemical trapping studies,⁴⁻⁶ demonstrating for the first time that single-photon photochemistry in the gas phase can stimulate multiple ligand loss. Perutz, Turner, Poliakoff, and several co-workers used IR spectroscopy to structurally characterize the photoproducts resulting from UV photodissociation of Group VIB hexacarbonyls trapped in low-temperature matrices.⁷⁻¹¹ Time-resolved infrared spectroscopy (TRIS) has been used, notably by Weitz and co-workers,¹²⁻¹⁵ Rosenfeld and co-workers,¹⁶⁻²² and Rayner and co-workers,²³⁻²⁸ to probe the UV photolysis of Group VIB hexacarbonyls in the gas phase. The C-O stretching frequencies of coordinatively unsaturated metal carbonyls generated in matrices provided the basis for assignment of gas-phase IR spectral features, from which it has been deduced that the symmetries of primary photoproducts generated in gas-phase experiments are identical to the symmetries of those species produced in low-temperature matrices. Furthermore, the gas-phase TRIS experiments have allowed us to develop a detailed understanding of energy disposal in excited photoproducts, collisional relaxation of rovibrational modes, metal-ligand bond dissociation energies, and the kinetics of ligand recombination with coordinatively unsaturated metal carbonyls.

In a recent review,²⁹ Weitz has pointed out the need for further studies into areas such as the electronic structure of coordinatively unsaturated organometallic species, mechanistic studies of gas-phase reactions thought to involve such species, and the influence of solvation on the kinetics and mech-

anism of these reactions. One might guess that multiphoton ionization (MPI) spectroscopy, coupled with mass spectrometric detection of the ionic photoproducts, would be a sensitive and specific probe of the excited electronic states of transient organometallic species. This technique has been used with a great deal of success in probing the structure of reactive organic radicals of fundamental significance.³⁰ The multiphoton excitation dynamics of $\text{Cr}(\text{CO})_6$ have been elucidated both by probing the distribution of electronic states of the Cr photoproduct³¹⁻³³ and by probing the kinetic energy release into intermediate (coordinatively unsaturated) molecular photoproducts.³⁴ For organometallic species in general, multiphoton dissociation (MPD) prevails over multiphoton up-pumping into bound neutral states. Consequently, complete ligand stripping (rather than resonant photoexcitation) dominates the neutral photochemistry, and atomic metal ions are often the *only* photoproducts observed in the MPI mass spectrum.³⁵ Due to the high degree of photolability of organometallic compounds in general, and transition metal carbonyls specifically, powerful techniques such as laser-induced fluorescence (LIF) and resonance Raman spectroscopy have not enjoyed general applicability to the study of the excited electronic states of coordinatively unsaturated species in the gas phase.³⁶

While the gas-phase photophysics of organometallic compounds is characterized by *multiple* ligand loss, the liquid-phase photophysics is characterized by *single* ligand loss.³⁷ Solvation of coordinatively unsaturated species occurs in solution on the picosecond timescale,³⁸ and the excess vibrational energy of the nascent photoproduct (which correlates, in gas phase photolysis, with further ligand loss) is rapidly disposed of amongst translational and internal modes of the surrounding solvent molecules. A fundamental question which arises is this: how does the photophysical behavior of an organometallic compound evolve from that of a naked molecule in the gas phase to that of a solvated molecule in the condensed phase? We can begin to explore the influence of solvation on photophysics by studying the photodissociation dynamics of transition metal coordination compounds contained within van der Waals clusters of solvent molecules. The properties of molecules within van der Waals clusters are often intermediate between those of the isolated molecule and those of the bulk phase, and the creation of reactive intermediates *within* these clusters allows us to model and probe condensed-phase pro-

cesses which might not otherwise be amenable to study.³⁹

It is not unreasonable to expect, *a priori*, that for sufficiently large van der Waals clusters of a solvated organometallic species, the photofragmentation dynamics may be so different from characteristic gas-phase behavior that MPI becomes an appropriate spectroscopic and dynamic probe. How large, though, is *sufficiently* large? We have recently reported the utility of MPI, coupled with mass spectrometry (MPI/MS), as a probe of the novel intracuster reactivity of coordinatively unsaturated Group VIB carbonyl photoproducts with their coordinatively saturated precursors within homogeneous clusters of metal hexacarbonyls.^{40,41} Based on the free-jet expansion conditions, we estimated that the neutral clusters we were probing were small, limited primarily to dimers, trimers, and perhaps tetramers.⁴¹

We have recently extended the scope of this work to studies of the multiphoton photophysics of van der Waals heteroclusters containing a single molecule of a transition metal coordination compound surrounded by a shell of solvent molecules. We now wish to ask what are the dynamical processes which eventually culminate in the MPI of these clusters. That is, what are the identities of the neutral species produced following intense UV irradiation, how effectively can multiphoton up-pumping (and subsequent *molecular* ionization) compete with photofragmentation (and subsequent *atomic* ionization), and how do the chemical identity of the solvent and the extent of solvation alter the observed dynamics? We report in this paper our preliminary results from a study of the multiphoton ionization of heteroclusters of $\text{Cr}(\text{CO})_6$ and methanol at 248 nm.

EXPERIMENTAL SECTION

Heteroclusters of $\text{Cr}(\text{CO})_6$ and methanol are formed in the free-jet expansion of a pulsed beam of seeded helium gas. The cluster beam passes through a collimating skimmer into a differentially pumped ion source, where it is irradiated by the mildly focused output of a KrF excimer laser. The resulting photoions are analyzed by time-of-flight mass spectrometry (TOFMS). The axes of the molecular beam, the ionizing laser pulse, and the ion flight tube are mutually perpendicular. The experimental apparatus is shown schematically in Figure 1, and its component parts are described below.

Mass spectrometer

The mass spectrometer is a commercially available time-of-flight mass spectrometer (R.M. Jordan Company) which has been designed especially for pulsed molecular beam sources. The spectrometer chamber is divided into two differentially pumped sections: a molecular beam chamber, and an ion source/flight tube chamber. The beam chamber is pumped by a 1400-1/sec 6" diffusion pump equipped with a liquid nitrogen cryobaffle, while the ion source and 1.5-m flight tube are pumped by a 330-1/sec turbopump. The ion source is surrounded by a gold-plated shroud which has apertures allowing free passage of both the molecular beam and the laser pulse through the center of the ionization region. The flight tube is surrounded by a liquid nitrogen-cooled jacket which is also in thermal contact with the gold-plated ion source shroud. This additional stage of cryopumping allows us to further minimize the pressure, and decrease the likelihood of ion-molecule collisions, in the flight tube and ionization region. The molecular beam can be monitored by a quadrupole residual gas analyzer (Dycor M200M) situated downstream from the neutral beam exit aperture of the ion source shroud. This feature allows us to monitor the alignment, chemical composition, and temporal profile of the pulsed molecular beam.

The ion source of the TOFMS is of the standard Wiley-McLaren three-grid configuration,⁴² with the extraction grids biased at high positive voltages and the final grid held at ground potential. The source is typically operated with an extraction field of 200 V/cm and an acceleration field of 1600

V/cm, yielding an ion beam with a nominal kinetic energy of about 4.25 keV. Mass resolution, $m/\Delta m$, under these conditions is about 200 to 250. A pair of transverse deflector plates immediately downstream from the ion source is floated symmetrically about 0 V dc, typically at a field strength between 30 and 50 V/cm, in order to compensate for the forward velocity of the molecular beam. Neglecting translationally hot photofragments, all of the nascent photoions will have a mean transverse component of velocity equal to that of the molecular beam. Since the transverse component of an ion's kinetic energy is proportional to its mass, ions arising from heavier neutrals in the molecular beam will have larger transverse kinetic energies, and the transmission efficiency of ions through the flight tube will display a mass dependence. In principle, this effect could be exploited in order to design a narrow-bandpass mass filter.

Photoion detection is accomplished with a low-impedance, dual microchannelplate detector operated in the analog mode. The detector is biased at a potential high enough to allow for sensitive detection of large (hundreds of amu) cluster ions, but low enough to prevent detector saturation and capacitive ringing: typically, -1800 to -2000 V dc. Transient saturation invariably occurs following arrival of the isotopes of Cr^+ (m/z 50, 52, 53, and 54); however, the detector recovers fully (as evidenced by the decay of capacitive ringing) within ca. 4 μsec , by the time ions of m/z 90 start to arrive. The unamplified signal from the microchannelplate detector is collected and averaged over 1000 laser pulses by a digital storage oscilloscope (LeCroy 9400).

Photoionization laser

The laser used to effect multiphoton ionization and dissociation of van der Waals heteroclusters in our experiment is a dual-cavity excimer laser (Lambda Physik EMG-150) operated on the KrF transition at 248 nm. We operate the laser in such a manner as to produce pulse energies around 100 millijoules, attenuating the output (if necessary) either by lowering the discharge voltage or by employing neutral density filters. The beam is then stopped down to a circular cross section 3 mm in diameter, and mildly focused by an S1-UV lens of 250-mm focal length to an intensity (within the center of the ion source) of about $2 \times 10^7 \text{ W/cm}^2$. Synchronization of the molecular beam pulse and the laser pulse is accomplished through the use of an external timing cir-

cut. By delaying the laser pulse 500 μ sec with respect to the beam valve solenoid pulse, we are able to sample clusters in that portion of the molecular beam where number density is large and cluster size distribution is very broad.

Molecular beam source

Heteroclusters of $\text{Cr}(\text{CO})_6$ solvated by methanol are formed in the free-jet expansion of a pulse of seeded helium gas. Helium gas (Linde, 99.995%) at a pressure of 18 psia is first passed through a gas purifier (Matheson 6406) to remove any traces of oxygen or water. The purified helium is then admitted into a glass trap containing methanol (Fisher, certified A.C.S.) at about 300 K and allowed to equilibrate. Finally, the methanol-saturated helium mixture is bled through a 1/4"-dia. U-tube containing $\text{Cr}(\text{CO})_6$ (Aldrich, 99%) and admitted into the low-volume stagnation region of a double-solenoid pulsed molecular beam valve (Newport Research Corporation BV-100, equipped with 0.5 mm-dia., 30° conical nozzle). The beam valve nozzle is situated about 100 nozzle diameters upstream from the skimmer on the ion source shroud. We typically operate the beam valve at a repetition rate of about 1 Hz. Under these conditions, maximum pressures in the beam chamber and ion source are 3×10^{-6} and 2×10^{-7} Torr, respectively; and base pressures between pulses are 8×10^{-7} and 6×10^{-8} Torr, respectively.

We are easily able to generate and detect heterocluster photoions containing as many as 100 methanol molecules. We therefore conclude that we are forming *neutral* heteroclusters at least as large, quite possibly larger, although we have no way of determining the extent of evaporation which takes place upon photoionization of large neutral heteroclusters. To ensure that the clusters we form are free of any contamination, it is essential that we carefully purify any components with which we seed our molecular beam. The $\text{Cr}(\text{CO})_6$ was purified initially by sublimation and sealed in a glass manifold under helium. The methanol was rendered free of any traces of acetone by treatment with NaOI^{43} and was then fractionally distilled and stored over molecular sieve 3A. Immediately prior to use, the methanol was rendered anhydrous by refluxing over and fractionally distilling from activated Mg turnings.⁴⁴ A few mL of distillate was collected and stored under helium in a sealed glass vessel connected to the beam valve manifold, while the remainder of the distillate was stored over CaH_2 in a stoppered flask. Both the methanol and the

$\text{Cr}(\text{CO})_6$ were degassed prior to operation of the molecular beam valve by several freeze-pump-thaw cycles.

Assignment of the identities of heterocluster photoions was greatly simplified by comparing the photoionization mass spectrum of $\text{Cr}(\text{CO})_6$ /methanol heteroclusters with that of $\text{Cr}(\text{CO})_6$ /methanol- d_4 heteroclusters. Methanol- d_4 (Aldrich, 99.5 atom % D) was purchased in sealed glass ampules and was used without any further purification, except for degassing. There was no detectable isotopic cross-contamination, even in the largest and most heavily solvated van der Waals cluster ions.

RESULTS AND DISCUSSION

Interpretation of the MPI mass spectra

The m/z ratios and assignments of ions observed in the MPI mass spectra of $\text{Cr(CO)}_6/\text{methanol}$ and $\text{Cr(CO)}_6/\text{methanol-d}_4$ van der Waals heteroclusters are listed in Table I. This tabulation represents a composite of data from several MPI mass spectra run under a variety of ion source voltages, and includes all major ions observed (except as noted in the caption). Relative intensities of these ions are not tabulated, since photoion yields across the mass range observed depend on both the laser fluence and the magnitude of the transverse deflector field. MPI of unclustered Cr(CO)_6 is expected to contribute to the total ion yield at the low end of the mass scale,⁴⁵ and we consequently observe significant amounts of CO^+ , singly and doubly charged chromium ions, and (to a lesser extent) Cr(CO)^+ . Photoionization of homogeneous methanol clusters in the molecular beam, followed by an intracuster bimolecular ion-molecule reaction,⁴⁶⁻⁴⁸ gives rise to a distribution of protonated methanol cluster ions. These cluster ions have very low relative yields, since the cross section for non-resonant photoionization of the homogeneous methanol clusters is much smaller than that for the metal carbonyl-containing heteroclusters. The protonated methanol cluster ions are translationally hotter than any of the other ions appearing in the mass spectrum, as evidenced by the comparative width of their time-of-arrival profiles. The broad kinetic energy distribution of these cluster ions may be a consequence of extensive monomer evaporation,⁴⁹ and/or isotropic ejection of methoxide radical, following the exothermic intracuster protonation reaction.

If the multiphoton ionization dynamics of solvated Cr(CO)_6 were rigorously analogous to those of naked Cr(CO)_6 , one would expect the heterocluster MPI mass spectrum to be dominated by solvated chromium ions, (i.e., S_nCr^+ , where $\text{S}=\text{CH}_3\text{OH}$). Based on the observed ion yields, however, we conclude that the ionization and fragmentation dynamics of solvated Cr(CO)_6 are *strikingly* different from those of the naked molecule. Portions of the mass spectra of $\text{Cr(CO)}_6/\text{methanol}$ and $\text{Cr(CO)}_6/\text{methanol-d}_4$ heteroclusters are shown in Figures 2 and 3, respectively. We observe comparable yields of S_nCr^+

and $S_n\text{Cr}(\text{CO})^+$ for all $n \geq 1$. Interestingly, we observe that the dominant feature of the mass spectrum is a repetitive sequence of peaks with the empirical formula, $S_n\text{Cr}(\text{CO})_x^+$ ($x = 0, 1, 2$), which first appears in the m/z range corresponding to $n + x = 6$. That is, the smallest stable ions in this sequence are those in which all the coordination sites of the metal center are occupied. For a given value of n , these cluster ions appear in a ratio, $x=0:x=1:x=2$, of approximately 1:2:4.

Several smaller peaks appear in both mass spectra which can be assigned to various binuclear cluster ions; that is, cluster ions containing more than one chromium atom. Since pressures in the ion source are low and ion residence times are short, these binuclear cluster ions do not arise from bimolecular association reactions of mononuclear cluster ions and mononuclear neutrals in the molecular beam but originate from the ionization of heteroclusters containing two (or more) molecules of $\text{Cr}(\text{CO})_6$. We note that we observe $S_n\text{Cr}_2^+$ only for $n = 0, 1$, and 2, but not for higher degrees of solvation. We also observe a minor sequence of peaks in the $\text{Cr}(\text{CO})_6$ /methanol heterocluster mass spectrum which starts at $m/z=312$, and repeats every 32 amu. Based on comparison with the deuterated heterocluster mass spectrum, we rule out the assignment of the cluster ions in this sequence as either $S_n\text{Cr}(\text{CO})_7^+$ or $S_n\text{Cr}_2\text{O}^+$. Instead, we tentatively assign these cluster ions as $S_n\text{Cr}_2(\text{CO})_4^+$, $n \geq 3$. (this assignment is tentative because of isobaric interference from solvated $\text{Cr}(\text{CO})_2^+$ in the deuterated heterocluster spectrum). The coordinatively unsaturated species, $\text{Cr}(\text{CO})_4$, is known to react with $\text{Cr}(\text{CO})_6$ at a rate near the gas-kinetic limit to form a binuclear product, probably $\text{Cr}_2(\text{CO})_{10}$,¹⁷ and we expect that such a process should also take place within a van der Waals cluster. Apparently, MPI of small heteroclusters of this binuclear product gives rise to solvated chromium dimer ions, whereas MPI of larger heteroclusters gives rise to binuclear cluster ions whose carbonyl ligands have not been completely stripped away.

While the MPI mass spectra of $\text{Cr}(\text{CO})_6$ /methanol and $\text{Cr}(\text{CO})_6$ /methanol- d_4 heteroclusters display several common features, they also display two prominent differences:

- 1) An additional minor sequence of peaks corresponding to $S_n\text{Cr}(\text{CO})_5^+$ appears for $n \geq 2$ in the mass spectrum of $\text{Cr}(\text{CO})_6$ / CH_3OH heteroclusters, as seen in Figure 2, yet is absent in the $\text{Cr}(\text{CO})_6$ / CD_3OD heterocluster spec-

trum as seen in Figure 3. However, the $S_n\text{Cr(CO)}_6^+$ ions which clearly appear in Figure 2 are also present in the spectrum of the deuterated heteroclusters, but manifest themselves as trailing shoulders on the more intense $S_n\text{Cr(CO)}_2^+$ peaks. Careful examination of Figure 3 reveals that the $S_n\text{Cr(CO)}_5^+$ ions, which should first appear at $m/z=264$ in the deuterated heterocluster spectrum, are conspicuously absent.

2) A minor sequence of cluster ions corresponding to $S_n\text{Cr(CO)}_3^+$ appears for $n \geq 9$ in the mass spectrum of $\text{Cr(CO)}_6/\text{CD}_3\text{OD}$ heteroclusters, but does not appear in the mass spectrum of $\text{Cr(CO)}_6/\text{CH}_3\text{OH}$ heteroclusters (Table I and Figure 3).

These two differences in observed ion yields in the two heterocluster MPI mass spectra *may* be a consequence of the dynamics of intracuster energy transfer in the ionic manifold. That is, CH_3OH and CD_3OD , by virtue of their differing vibrational frequencies, are expected to have different efficiencies for V-V cooling of a nascent, vibrationally hot photoion, (i.e., $[\text{Cr(CO)}_{x \leq 6}]^+$). Whereas MPI of a vibrationally relaxed neutral molecule may give rise to a stable photoion, MPI of a hot neutral may yield a vibrationally excited photoion. Depending on the degree of vibrational excitation of the photoion and the electronic structure in the ionic manifold, predissociation of hot photoions may occur at a rate so fast as to preclude their detection. Consequently, the appearance of cluster ions in the mass spectrum may be influenced not only by the identities of the neutral solvated photoproducts, but also by the internal energies of these photoproducts,⁵⁰ and by the efficiency with which the internal energy of the resultant photoion can be quenched by surrounding solvent molecules.

Nature of the photofragmentation dynamics

We now consider, in a qualitative manner, the photophysics of van der Waals clusters containing Cr(CO)_6 . We would like to develop an understanding of the photofragmentation dynamics of solvated Cr(CO)_6 , the photoionization dynamics of the solvated neutral photoproducts, and the competition between fragmentation and ionization. We will first examine several possible dynamical descriptions of cluster excitation, and consider the implications for observed photoion yields. We will then attempt to reconcile the predictions of these various schemes with our mass spectrometric results.

The simplest alternative to consider is that MPI of Cr(CO)_6 -containing clusters proceeds in a manner analogous to that of naked, unclustered Cr(CO)_6 . That is, the solvated Cr(CO)_6 undergoes complete ligand stripping, and the resulting solvated metal atom is subsequently photoionized. In such a case, we would expect the MPI mass spectrum to be dominated by solvated metal ions, S_nCr^+ , with little (if any) contribution from solvated molecular ions, $\text{S}_n\text{Cr(CO)}_x^+$ ($x \leq 6$). Clearly, such a scheme does not describe the multi-photon dissociation and ionization dynamics of these clusters, since the solvated chromium ions do not dominate the MPI mass spectrum, and the solvated molecular ions do not represent merely a minor contribution. Consequently, we must consider another alternative dynamical scheme.

A second alternative is that photofragmentation of Cr(CO)_6 within these clusters can be described by usual liquid-phase dynamics. Photofragmentation of coordination compounds in the liquid phase is characterized by loss of a single ligand, independent of photon energy.³⁷ If photofragmentation of Cr(CO)_6 within van der Waals clusters were limited to loss of a single CO ligand, then we would expect that the neutral cluster population following photolysis would consist of $\text{S}_n\text{Cr(CO)}_5$ (as well as any $\text{S}_n\text{Cr(CO)}_6$ which did not dissociate), and that $\text{S}_n\text{Cr(CO)}_6^+$ and $\text{S}_n\text{Cr(CO)}_5^+$ would therefore be the *primary* photoions.⁵¹ Furthermore, if photofragmentation in the neutral manifold were truly limited to single ligand loss, we would expect the observed photoion yields to be insensitive to the laser wavelength. We have recently discovered, however, that the photoion yields from MPI of Cr(CO)_6 /methanol heteroclusters display a very *strong* wavelength dependence.⁵² Whereas excitation of these heteroclusters at 248 nm (corresponding primarily to the $^1\text{A}_{1g} \rightarrow ^1\text{T}_{1u}$ MLCT transition³⁴) gives rise to photoions such as those shown in the mass spectra in Figures 2 and 3, excitation around 350 nm (corresponding to the $^1\text{A}_{1g} \rightarrow ^1\text{T}_{1g}$ LF transition³⁷) gives rise exclusively to solvated Cr(CO)_5^+ cluster ions. These observations are inconsistent with a dynamical scheme in which photofragmentation in the neutral manifold is wavelength-independent and limited to loss of just a single ligand.

We can, however, account for the observed wavelength dependence of the photoion yields if we assume that the extent of photofragmentation within the neutral manifold is also dependent on wavelength. This kind of photofragmentation behavior is certainly not typical of transition metal coordination

compounds dissolved in solution, but is analogous rather to the single-photon photofragmentation behavior of gas-phase species. The cluster ions we observe in the mass spectrum must therefore arise via non-resonant MPI of the solvated neutral species, Cr(CO)_x ($x \leq 6$), and subsequent fragmentation of the primary photoions. These dynamics are unusual for an organometallic species, since MPI in this case appears to compete effectively with (and perhaps prevail over) MPD. To more quantitatively characterize these dynamics, we would like to determine the values that x takes on; that is, we wish to identify *all* of the neutral species which are undergoing MPI and contributing to the observed photoion yields. While the present experiments do not allow us to unambiguously identify such species, we can certainly identify *reasonable* candidates based on our knowledge of Cr(CO)_6 photophysics at both the low-pressure (collisionless) and high-pressure (condensed phase) limits.

Photofragmentation in the neutral manifold

Let us now consider limiting cases for photodissociation of Cr(CO)_6 . Energetics for the dissociation of Cr(CO)_6 to neutral photoproducts are represented in Figure 4. Ground-state Cr(CO)_6 is placed at the origin, and the coordinatively unsaturated photoproducts are placed according to their known or estimated bond dissociation energies. Bond dissociation energies for the first and second carbonyl ligands (BDE1 and BDE2) are taken from the RRKM calculations of Fletcher and Rosenfeld,¹⁹ BDE3 is estimated from the photofragment recoil velocity analyses of Vernon and co-workers,⁵³ and the remaining BDE's are taken as an average value such that the sum of the six BDE's equals the heat of disruption determined by Pilcher *et al.*⁵⁴

Tyndall and Jackson have recently examined the photodissociation of Cr(CO)_6 in a molecular beam following irradiation at 248 nm, using low-energy electron impact mass spectrometry to monitor the primary and secondary neutral photoproducts.⁵⁵ Based on the laser intensity dependence of the product ion signals, they proposed the following scheme for sequential photodissociation at 248 nm under collisionless conditions:



Here, Cr(CO)_4^* denotes an internally excited photoproduct. Tyndall and

Jackson estimated, based on RRKM calculations, that the internal energy of the $\text{Cr}(\text{CO})_4$ may be as high as 38 kcal/mol.⁵⁶ Based on a kinetic rate equation analysis of the photoproduct yields, they determined photodissociation cross sections for reactions (1) and (2) (σ_1 and σ_2) of $5.6 \times 10^{-17} \text{ cm}^2$ and $1.5 \times 10^{-16} \text{ cm}^2$, respectively. They also described a direct, non-sequential process³³ in which $\text{Cr}(\text{CO})_6$ is excited into a dissociative continuum via two- or three-photon absorption, giving rise to several excited states of atomic chromium:



This process is important at higher fluences, although no photodissociation cross sections were reported.

The dynamics of UV photodissociation of $\text{Cr}(\text{CO})_6$ in solution, and subsequent solvent coordination by nascent $\text{Cr}(\text{CO})_5$, have been extensively studied. Differences in the electronic spectra of naked and solvent-coordinated $\text{Cr}(\text{CO})_5$ have been exploited in the picosecond and sub-picosecond transient visible absorption experiments of Joly and Nelson,⁵⁷ Lee and Harris,⁵⁸ and Simon and Xie.⁵⁹⁻⁶² The temporal resolution of transient vibrational spectroscopy is limited by the width of the probe pulse and the speed of the detector; hence, typical TRIS techniques, utilizing CW IR sources and relatively slow detectors, have not been suitable for the study of fast solution-phase dynamics. However, several schemes have been devised to overcome the inherent limitations of transient IR absorption techniques. Spears and co-workers have employed a fast (20 psec) IR probe pulse in a transient IR absorption study of the UV photodissociation of $\text{Cr}(\text{CO})_6$ in cyclohexane⁶³ and THF.⁶⁴

Hochstrasser and co-workers have obtained picosecond and better resolution in a diode laser absorption experiment by sum-frequency mixing of a fast visible pulse with the transmitted IR, with subsequent detection by a fast visible-light detector.⁶⁵ Hopkins and co-workers have employed transient Stokes and anti-Stokes resonant Raman spectroscopy to probe photodissociation and solvent coordination dynamics in solution on the picosecond timescale.⁶⁶

Results from the transient visible absorption experiments are consistent with the following scheme for the photodissociation of $\text{Cr}(\text{CO})_6$ in solution:





Here, S denotes a solvent molecule, and the asterisk once again denotes an internally excited species. Reaction (4) corresponds to excitation of ground-state Cr(CO)_6 into the first excited singlet state. Calculations at the ab initio SCF-CI level⁶⁷ predict that this surface correlates with the first excited singlet surface of C_{4v} Cr(CO)_5 , so the Cr(CO)_5^* photoproduct should appear in its first excited singlet state. It is thought to relax via Jahn-Teller distortion to D_{3h} symmetry, internal conversion to the singlet ground state of the D_{3h} species, and distortion back to a vibrationally hot C_{4v} species in the ground electronic state. Electronic relaxation may take place before, during, or after the solvent coordination step represented in reaction (6). Simon and Xie suggest that electronic relaxation of Cr(CO)_5^* precedes solvent coordination.⁵⁸ Transients observed in both the visible absorption⁵⁸ and Raman⁶⁶ experiments have been interpreted in terms of slow vibrational relaxation of $\text{S} \cdot \text{Cr(CO)}_5^*$, represented in reaction (7), which takes place on a timescale of tens of picoseconds to a few hundred picoseconds, depending on the identity of the solvent.

Joly and Nelson have followed the UV photodissociation of Cr(CO)_6 in methanol via transient visible absorption spectroscopy.⁵⁷ Their instrumental response time in this study, as determined from cross-correlation of the UV pump and visible probe pulses, is 95 femtoseconds. They report that CO loss, represented by reactions (4) and (5), takes place within 0.3 psec of the absorption of the UV photon. Solvent coordination is complete within 1.6 psec, while vibrational relaxation is complete within 70 psec. Apparently, both tetrahydrofuran and cyclohexane are more efficient than methanol at vibrationally cooling the solvent-coordinated pentacarbonyl, since the vibrationally cold photoproduct of reaction (7) appears in both of these cases within 50 (rather than 70) psec.

The multiphoton dissociation dynamics of Cr(CO)_6 in solution have not been rigorously investigated. However, single- and multiphoton dissociation processes of matrix-isolated Group VIB hexacarbonyls have been well-characterized. The primary photoproduct of UV or visible single-photon photolysis of M(CO)_6 ($\text{M} = \text{Cr, Mo, W}$) in hydrocarbon glasses at 77 K or rare gas matrices at

20 K is the corresponding metal pentacarbonyl of C_{4v} symmetry.⁹ More highly unsaturated secondary photoproducts, $M(CO)_x$ ($x = 2, 3, 4$), result from subsequent absorption of an additional photon by the corresponding $M(CO)_{x+1}$.¹⁰



Each photon absorbed results in the loss of a single CO ligand, so that formation of $M(CO)_2$ from $M(CO)_6$, for example, would require sequential absorption of four photons.

We have now considered the single- and multiphoton dissociation of $Cr(CO)_6$ at two extremes: the low-pressure, collisionless regime, and the high-pressure, condensed-phase regime. What does the behavior of $Cr(CO)_6$ at these two extremes imply regarding photodissociation within van der Waals heteroclusters, and how will the photodissociation dynamics of these *neutral* heteroclusters be reflected in the observed *photoion* yields? We might imagine two limiting cases for the appearance of heterocluster photoions, as generalized in Figure 5. In this scheme, photodissociation (in either the neutral or ionic manifold) occurs down the length of a column through sequential absorption of photons, while photoionization of a given species occurs via multiphoton absorption in the horizontal direction. One possible explanation which accounts for the observed photoion yields is that the neutral clusters formed in the molecular beam expansion are *first* photoionized, then *subsequently* photodissociated. Alternatively, dissociation of these neutral clusters may take place initially, and photoionization of the solvated neutral fragments may follow. We consider these two alternatives below.

One limiting case we can imagine is that $S_n Cr(CO)_6^+$ is the *one and only* primary photoion; that is, all ions arise through initial ionization of the coordinatively saturated species, $S_n Cr(CO)_6$, followed by subsequent photofragmentation in the *ionic* manifold. The electron impact ionization of $Cr(CO)_6$ is thought to take place in such a fashion.⁶⁸ If we assume that the photoionization and fragmentation of these heteroclusters is accurately described by such a model, and further assume that photofragmentation in the ionic manifold occurs statistically, we can make two predictions about photoion yields. First, by virtue of the statistical assumption, the photofragmentation branching ratios (within the ionic manifold) will depend on the *total*

photon energy absorbed in a multiphoton process by the $S_n\text{Cr}(\text{CO})_6^+$ parent ion, rather than the energy of a *single* photon of the wavelength at which the parent ion is irradiated. This means that the observed photoion yields and branching ratios will depend on the photodissociation cross section of the parent ion at the photoionizing laser's wavelength, and the fluence of the laser. Furthermore, yields and branching ratios will *not* depend explicitly on the wavelength at which the parent ion is irradiated. A second prediction we can make is that at sufficiently high laser fluence, we should be able to drive photofragmentation of the parent ion toward complete ligand stripping, regardless of laser wavelength, and that the observed photoions in this case should correspond primarily to solvated chromium ions, $S_n\text{Cr}^+$. Neither of these two predictions are born out in our observations from the present experiments at 248 nm, or other experiments at wavelengths to the red.⁵² We find instead that the photoion branching ratios are *quite* wavelength-dependent, and that photoion fragmentation at high fluence (strong focusing) is not necessarily driven to complete ligand loss. Our observations are inconsistent with a dynamical model in which photodissociation takes place exclusively within the ionic manifold. We must therefore conclude that the heterocluster photoions we observe *do not* arise solely through initial photoionization of the solvated hexacarbonyl, $S_n\text{Cr}(\text{CO})_6$, followed by subsequent fragmentation of the incipient parent ion.

We now consider an alternative dynamical model, where photodissociation within the neutral manifold takes place first, and ionization takes place subsequently. At the extreme limit, we might imagine that the dynamics resemble those of matrix-isolated $\text{Cr}(\text{CO})_6$. In such a case, single-photon absorption would result in single-ligand loss, regardless of photon wavelength, and multiply unsaturated neutral species would result from sequential one-photon absorption steps. The various photoions would then arise through non-resonant MPI of the ensemble of neutral photoproducts. One would expect that if photodissociation in the neutral manifold were wavelength-independent, then the observed photoion yields might also be wavelength-independent. However, since this expectation runs counter to the results of our other studies,⁵² we suggest that photodissociation within the neutral manifold is, in fact, wavelength-dependent, much like the photodissociation of naked $\text{Cr}(\text{CO})_6$ in the gas phase. We suggest the following *specific* scheme for the multiphoton dis-

sociation and ionization dynamics of $\text{Cr(CO)}_6/\text{methanol}$ heteroclusters at 248 nm, illustrated in Figure 6. In this scheme, the left-most column represents products of photodissociation within the neutral manifold; the central column represents the *nascent* photoions, which we assume are internally excited (*vide infra*); and the right-most column represents the *observed* photoions. The nascent, internally excited photoions may predissociate by corresponding rates (or sets of rates), k_1 and $\{k_3\}$. They may also internally relax by the corresponding rates, $k_2[\text{S}]$ and $k_4[\text{S}]$. Presumably, such relaxation can take place via intracluster V-V energy transfer from $[\text{Cr(CO)}_x]^+$ to S. The efficiency of such a process will depend on the proper correlation of vibrational motions and frequencies between the excited ion and the adjacent solvent molecule. Different solvents might therefore effect V-V cooling at different rates. Two important caveats should be kept in mind. First, since we are unable to assess the extent to which solvent evaporation (i.e., changes in the index n) takes place during photoionization or photodissociation, we cannot comment on the relative efficiency of evaporative cooling as a means of relaxing the internal modes of excited photoproducts. Second, although we have not explicitly included photofragmentation pathways within the ionic manifold, we do not mean to imply that such pathways do not exist. We shall discuss subsequent ionic photofragmentation in more detail below, after first considering some estimates of the energetics in the ionic manifold.

One- and two-photon photodissociation of Cr(CO)_6 under collisionless conditions has been examined by Tyndall and Jackson⁵⁵ (*vide supra*). By analogy with their gas-phase work, we take the two photodissociation cross sections in the neutral manifold in Figure 6 as equal to the corresponding cross sections in reactions (1) and (2). Likewise, we assume that the primary neutral photoproduct, $\text{S}_n\text{Cr(CO)}_4^*$, has an internal energy of ≈ 38 kcal/mol. Considering the energetics of photodissociation in the neutral manifold, as shown in Figure 4, we would also expect the secondary photoproduct to be internally excited to a large extent. However, we have not attempted to separate the set of decay rates, $\{k_5\}$, for the nascent ion of this photoproduct into predissociation rates and vibrational cooling rates. Since we do not know the absolute value of σ_B , the photoionization cross section for $\text{S}_n\text{Cr(CO)}_4^*$, we are not able to estimate the importance of secondary photodissociation *vis a vis* photoionization. However, we expect that if the photoionization of $\text{S}_n\text{Cr(CO)}_4^*$

is truly a two-photon process, the branching ratio of photoionization to secondary photodissociation should go as $\sigma_B I^2 / \sigma_2 I$, and photoionization should eventually dominate at high laser intensities.

Photoion yields

Ionization potentials for the coordinatively unsaturated species, $\text{Cr}(\text{CO})_x$ ($x \leq 5$), are unknown, but the ionization potential for $\text{Cr}(\text{CO})_6$ as well as some bond dissociation energies for neutral species are known. If we estimate bond dissociation energies for the corresponding ionic species from mass spectral appearance potentials,⁶⁸⁻⁷⁰ we may then obtain thermochemical estimates for ionization potentials of the unsaturated neutral species. These estimates must be taken with a great deal of caution, since reported appearance potentials vary considerably. The thermochemical data thus obtained are summarized in Table II, and a graphical representation of the energetics of photodissociation within the ionic manifold is shown in Figure 7. As a zeroth-order assumption, we will take the ionization potentials and BDE's of the naked species listed in Table II as equal to the values for the corresponding solvated species in Figure 6.

We will now draw upon the thermochemical estimates from Table II in order to account for production of the proposed *nascent* photoions, shown in the central column of Figure 6, as well as the *observed* photoions, shown in the right-most column. Consider first the species, $S_n[\text{Cr}(\text{CO})_6^*]^+$. Based on the known ionization potential for $\text{Cr}(\text{CO})_6$,⁷¹ we estimate an upper limit to the internal energy of the nascent photoion, $S_n[\text{Cr}(\text{CO})_6^*]^+$, of about 2 eV. Based on the He I α photoelectron spectrum of $\text{Cr}(\text{CO})_6$, we estimate a lower limit to the internal energy of about 0.4 eV. The rate constant, k_1 , for predissociation of this ion is apparently small enough (compared with $k_2[\text{CH}_3\text{OH}]$) so that both $S_n\text{Cr}(\text{CO})_6^+$ and $S_n\text{Cr}(\text{CO})_5^+$ are observed in the MPI mass spectrum of $\text{Cr}(\text{CO})_6/\text{CH}_3\text{OH}$ heteroclusters. Subsequent one-photon absorption by either of these cluster ions, to the extent that it occurs, probably gives rise to $S_n\text{Cr}(\text{CO})_x^+$ ($x \leq 2$). We suggest that V-V energy transfer to CH_3OH is not efficient enough to completely cool the nascent $S_n[\text{Cr}(\text{CO})_6^*]^+$. However, V-V energy transfer to CD_3OD must occur so efficiently that $k_2[\text{S}] \gg k_1$. Hence, the nascent $S_n[\text{Cr}(\text{CO})_6^*]^+$ which arises from MPI of $\text{Cr}(\text{CO})_6/\text{CD}_3\text{OD}$ heteroclusters is rapidly cooled, and $S_n\text{Cr}(\text{CO})_5^+$ is consequently absent from the spec-

trum of the deuterated heteroclusters.

We note that according to our thermochemical estimates, ionization of the primary neutral photoproduct, $S_n\text{Cr}(\text{CO})_4^*$, even after taking into account its internal energy, will require absorption of at least two photons. Tyndall and Jackson have inferred that low-energy electron impact ionization of the unclustered analog, $\text{Cr}(\text{CO})_4^*$, gives rise to a nascent ion which is internally excited to such an extent that it promptly fragments to $\text{Cr}(\text{CO})_x^+$ ($x \leq 2$).⁵⁵ If the production, via electron impact ionization, of this internally excited ion is controlled primarily by Franck-Condon factors, then we might expect non-resonant photoionization to also give rise to an excited ion through a vertical transition. This nascent photoion would be expected to predissociate, given sufficient internal energy and favorable overlap with a repulsive surface. In light of this, our assumption that the nascent $S_n[\text{Cr}(\text{CO})_4^*]^+$ promptly fragments to smaller photoions seems justified. This accounts for our failure to observe photoions corresponding to $S_n\text{Cr}(\text{CO})_4^+$. Subsequent one-photon absorption by $\text{Cr}(\text{CO})_x^+$ ($x \leq 2$) undoubtedly occurs, leading to additional fragmentation and/or evaporation. Once again, we suggest that V-V energy transfer to CH_3OH is not efficient, but that V-V energy transfer to CD_3OD is apparently efficient enough such that $k_4[\text{S}]$ is comparable to rate constants in the set, $\{k_3\}$. This accounts for our ability to observe $S_n\text{Cr}(\text{CO})_3^+$ *only* in the MPI mass spectrum of the $\text{Cr}(\text{CO})_6/\text{CD}_3\text{OD}$ heteroclusters, but *not* in the spectrum of the $\text{Cr}(\text{CO})_6/\text{CH}_3\text{OH}$ heteroclusters.

As mentioned above, we are unable to assess the significance of the secondary photoproduct, $S_n\text{Cr}(\text{CO})_2^*$, within the photodissociation dynamics in the neutral manifold. We are therefore unable to estimate the extent to which ionization of $S_n\text{Cr}(\text{CO})_2^*$ contributes to the observed photoion yields. We can say, however, that at high laser intensity, the ionization of $S_n\text{Cr}(\text{CO})_4^*$ *should* dominate over secondary photodissociation. Any $S_n\text{Cr}(\text{CO})_2^*$ which *does* appear under these circumstances should ultimately represent only a minor contribution to the total ion current.

Ramifications of the present studies

The results of the experiments described herein suggest that multiphoton ionization spectroscopy is a useful and direct probe of the photodissociation and solvation dynamics of transition metal coordination compounds

within small van der Waals clusters in the gas phase. Several implications for the further study of coordination compounds are readily apparent. We describe three such areas below.

Little is known regarding the electronic structure of coordinatively unsaturated organometallic species; however, we believe that by using a two-color technique, we will be able to undertake such spectroscopic studies. By judiciously selecting the proper wavelength and fluence for photodissociation, we should be able to prepare specific (at best, *individual*) coordinatively unsaturated species within clusters; and by employing a tunable photoionization laser, we should be able to study excited electronic states of the selected species by resonance-enhanced MPI (REMPI). We have already initiated a study of the photodissociation and ionization dynamics of $\text{Cr}(\text{CO})_6/\text{methanol}$ heteroclusters in the spectral region corresponding to the lowest ligand field transition, and have used a one-color REMPI probe to demonstrate that the principle sequence of cluster ions does *not* arise from initial ionization of either methanol or atomic chromium. This work is described elsewhere.⁵²

The production of coordinatively unsaturated species in solution, the dynamics of solvent coordination, and the specifics of intermolecular energy transfer and relaxation are processes of great interest in the study of solution-phase organometallic chemistry. Unsaturated coordination compounds within van der Waals clusters of solvent molecules are amenable to investigation by powerful molecular beam and gas-phase spectroscopic techniques, and they should serve as excellent experimental models for the study of condensed-phase processes. These processes are extremely fast, and if we can determine (or at least estimate) the relevant photodissociation and photoionization cross sections, we can in principle control the timescale of the experiment not only by specifying the *temporal* characteristics of the photon sources, but by specifying their *intensities* as well. The *mass-selective* nature of such cluster REMPI experiments should allow us access to information not easily obtainable with less-specific absorption spectroscopic probes.

There is no reason we must restrict the scope of our MPI studies to heteroclusters containing unreactive solvent molecules. Many coordinatively unsaturated organometallic species are thought to be important in catalytic mechanisms, and some interesting experiments can be devised wherein the solvent molecules within the heterocluster are actually substrates for the photo-

generated catalyst. One could then follow not only the decay of substrate and appearance of product, but also the catalytic species itself. Such studies might substantially increase our understanding of mechanistic organometallic chemistry.

CONCLUSIONS

We have examined the 248-nm multiphoton dissociation and ionization dynamics of van der Waals heteroclusters of $\text{Cr}(\text{CO})_6$ and methanol generated in a pulsed free-jet expansion of seeded helium. We find that the multiphoton photophysics of $\text{Cr}(\text{CO})_6$ solvated within van der Waals clusters is strikingly different from that of the naked molecule in the gas phase. We observe two principle series of cluster ions: a minor series corresponding to $\text{S}_n\text{Cr}(\text{CO})_x^+$ ($x = 5, 6$), which first appears in the mass spectrum at $n + x = 7$; and a major series corresponding to $\text{S}_n\text{Cr}(\text{CO})_x^+$ ($x = 0, 1, 2$), which first appears in the mass spectrum at $n + x = 6$. We note that these photoion yields are highly wavelength dependent, and we propose a dynamical scheme accounting for the observed photoions in which the behavior of the solvated $\text{Cr}(\text{CO})_6$ molecule toward photodissociation and ionization is intermediate between gas-phase and condensed-phase behavior. Differences in relative photoion yields between the MPI mass spectrum of $\text{Cr}(\text{CO})_6/\text{CH}_3\text{OH}$ clusters and the MPI mass spectrum of $\text{Cr}(\text{CO})_6/\text{CD}_3\text{OD}$ clusters are attributed to a dynamical effect. It is proposed that a nascent, internally excited photoion will tend to predissociate unless relaxed by V-V energy transfer to an adjacent solvent molecule within the cluster. CD_3OD appears to more efficiently cool the internally excited photoion than does CH_3OH , due presumably to a more favorable correlation of vibrational motions and frequencies with the nascent photoion. Consequently, ionic predissociation takes place to a lesser extent following photoionization of $\text{Cr}(\text{CO})_6/\text{CD}_3\text{OD}$ heteroclusters. The application of resonance-enhanced MPI to the study of mixed van der Waals clusters of coordination compounds will allow us to probe the upper excited electronic states of coordinatively unsaturated species, the dynamics of solvation and condensed-phase energy transfer processes, and the mechanisms of organometallic catalytic reactions.

ACKNOWLEDGMENT

We gratefully acknowledge the financial support of this work provided by the Office of Naval Research.

REFERENCES

- (1) R. Hoffmann, *Angew. Chem., Intl. Ed. Engl.* **21**, 711 (1982).
- (2) T.J. Meyer and J.V. Caspar, *Chem. Rev.* **85**, 187 (1985).
- (3) M. Poliakoff and E. Weitz, *Adv. Organomet. Chem.* **25**, 277 (1986).
- (4) G. Nathanson, B. Gitlin, A.M. Rosan, and J.T. Yardley, *J. Chem. Phys.* **74**, 361 (1981).
- (5) J.T. Yardley, B. Gitlin, G. Nathanson, and A.M. Rosan, *J. Chem. Phys.* **74**, 370 (1981).
- (6) W. Tumas, B. Gitlin, A.M. Rosan, and J.T. Yardley, *J. Am. Chem. Soc.* **104**, 55 (1982).
- (7) M.A. Graham, R.N. Perutz, M. Poliakoff, and J.J. Turner, *J. Organomet. Chem.* **34**, C34 (1972).
- (8) R.N. Perutz and J.J. Turner, *Inorg. Chem.* **14**, 262 (1975).
- (9) R.N. Perutz and J.J. Turner, *J. Am. Chem. Soc.* **97**, 4791 (1975).
- (10) R.N. Perutz and J.J. Turner, *J. Am. Chem. Soc.* **97**, 4800 (1975).
- (11) J.K. Burdett, M.A. Graham, R.N. Perutz, M. Poliakoff, A.J. Rest, J.J. Turner, and R.F. Turner, *J. Am. Chem. Soc.* **97**, 4805 (1975).
- (12) A. Ouderkirk and E. Weitz, *J. Chem. Phys.* **79**, 1069 (1983).
- (13) A. Ouderkirk, P. Werner, N.L. Schultz, and E. Weitz, *J. Am. Chem. Soc.* **105**, 3354 (1983).
- (14) T.A. Seder, S.P. Church, A.J. Ouderkirk, and E. Weitz, *J. Am. Chem. Soc.* **107**, 1432 (1985).
- (15) T.A. Seder, S.P. Church, and E. Weitz, *J. Am. Chem. Soc.* **108**, 4721 (1986).
- (16) T.R. Fletcher and R.N. Rosenfeld, *J. Am. Chem. Soc.* **105**, 6358 (1983).
- (17) T.R. Fletcher and R.N. Rosenfeld, *J. Am. Chem. Soc.* **107**, 2203 (1985).
- (18) T.R. Fletcher and R.N. Rosenfeld, *J. Am. Chem. Soc.* **108**, 1686 (1986).
- (19) T.R. Fletcher and R.N. Rosenfeld, *J. Am. Chem. Soc.* **110**, 2097 (1988).
- (20) J.P. Holland and R.N. Rosenfeld, *Chem. Phys. Lett.* **145**, 481 (1988).
- (21) J.P. Holland and R.N. Rosenfeld, *J. Chem. Phys.* **89**, 7217 (1988).
- (22) J.A. Ganske and R.N. Rosenfeld, *J. Phys. Chem.* **93**, 1959 (1989).
- (23) Y. Ishikawa, R.A. Weersink, P.A. Hackett, and D.M. Rayner, *Chem. Phys. Lett.* **142**, 271 (1987).
- (24) Y. Ishikawa, P.A. Hackett, and D.M. Rayner, *Chem. Phys. Lett.* **145**, 429 (1988).

- (25) Y. Ishikawa, C.E. Brown, P.A. Hackett, and D.M. Rayner, *Chem. Phys. Lett.* **150**, 506 (1988).
- (26) Y. Ishikawa, P.A. Hackett, and D.M. Rayner, *J. Mol. Struct.* **174**, 113 (1988).
- (27) Y. Ishikawa, P.A. Hackett, and D.M. Rayner, *J. Phys. Chem.* **92**, 3863 (1988).
- (28) Y. Ishikawa, C.E. Brown, P.A. Hackett, and D.M. Rayner, *J. Phys. Chem.* **94**, 2404 (1990).
- (29) E. Weitz, *J. Phys. Chem.* **91**, 3945 (1987).
- (30) J.W. Hudgens in *Advances in Multiphoton Processes and Spectroscopy*, Vol. 4; S.H., Lin, Ed.; World Scientific Publishing Company: Singapore, 1988.
- (31) D.P. Gerrity, L.J. Rothberg, and V. Vaida, *J. Phys. Chem.* **87**, 2222 (1983).
- (32) G.W. Tyndall and R.L. Jackson, *J. Am. Chem. Soc.* **109**, 582 (1987).
- (33) G.W. Tyndall and R.L. Jackson, *J. Chem. Phys.* **89**, 1364 (1988).
- (34) B. Venkataraman, H. Hou, Z. Zhang, S. Chen, G. Bandukwalla, and M. Vernon, *J. Chem. Phys.* **92**, 5338 (1990).
- (35) W.E. Hollingsworth and V. Vaida, *J. Phys. Chem.* **90**, 1235 (1986).
- (36) Transient vibrational and electronic absorption spectroscopies with picosecond temporal resolution have been used recently to probe the liquid-phase UV photolysis of $\text{Cr}(\text{CO})_6$, and the vibrational relaxation and solvation dynamics of solvated $\text{Cr}(\text{CO})_5$ (vide infra).
- (37) G.L. Geoffroy and M.S. Wrighton, *Organometallic Photochemistry*; Academic: New York, 1979.
- (38) J.A. Welch, K.S. Peters, and V. Vaida, *J. Phys. Chem.* **86**, 1941 (1982).
- (39) W.R. Peifer, M.T. Coolbaugh, and J.F. Garvey in *Clusters and Clustering from Atoms to Fractals*; P. Reynolds, Ed.; North-Holland: Amsterdam, 1990.
- (40) W.R. Peifer and J.F. Garvey, *J. Phys. Chem.* **93**, 5906 (1989).
- (41) W.R. Peifer and J.F. Garvey, "Multiphoton Ionization of Group VIB Hexacarbonyl van der Waals Clusters: Trends in Intracuster Photochemistry", *Int. J. Mass Spectrom. Ion Proc.* (1990) in press.
- (42) W.C. Wiley and I.H. McLaren, *Rev. Sci. Instrum.* **26**, 1150 (1955).
- (43) H.H. Bates, J.M. Mullaly, and H. Hartley, *J. Chem. Soc.* **123**, 401 (1923).
- (44) H. Lund and J. Bjerrum, *Ber. Deut. Chem. Gesell.* **64**, 210 (1931).
- (45) M.A. Duncan, T.G. Dietz, and R.E. Smalley, *Chem. Phys.* **44**, 415 (1979).

- (46) S. Morgan and A.W. Castleman, Jr., J. Am. Chem. Soc. **109**, 2867 (1987).
- (47) S. Morgan and A.W. Castleman, Jr., J. Phys. Chem. **93**, 4544 (1989).
- (48) S. Morgan, R.G. Keesee, and A.W. Castleman, Jr., J. Am. Chem. Soc. **111**, 3841, (1989).
- (49) U. Buck, personal communication.
- (50) For a discussion of the effects of internal energy of the neutral molecule on the mass spectral fragmentation pattern, see: A. Danon, A. Amirav, J. Silberstein, I. Salman, and R.D. Levine, J. Phys. Chem. **93**, 49 (1989).
- (51) The observed photoions would, of course, consist of solvated Cr(CO)_6^+ and solvated Cr(CO)_5^+ cluster ions, and/or their daughter photofragment ions. We would expect fragmentation of the primary photoions to be a statistical process. See: J. Silberstein and R.D. Levine, Chem. Phys. Lett. **74**, 6 (1980).
- (52) W.R. Peifer and J.F. Garvey, "Wavelength Dependence of the Multiphoton Ionization and Fragmentation Dynamics of $\text{Cr(CO)}_6/\text{Methanol}$ van der Waals Heteroclusters" J. Phys. Chem. (1990) submitted.
- (53) The experiment of Vernon and co-workers (Ref. 34) is sensitive to the sum, $\text{BDE1} + \text{BDE2} + \text{BDE3}$. We subtract from their optimized sum the values of BDE1 and BDE2 (Ref. 19) to arrive at an estimate for BDE3.
- (54) G. Pilcher, M.J. Ware, and D.A. Pittman, J. Less-Common Metals **42**, 223 (1975).
- (55) G.W. Tyndall and R.L. Jackson, J. Chem. Phys. **91**, 2881 (1989).
- (56) Fletcher and Rosenfeld originally calculated that the Cr(CO)_4^+ internal energy is ≤ 23 kcal/mol (Ref. 17). This calculation is based on an estimated $(\text{CO})_4\text{Cr-CO}$ bond dissociation energy of 40 kcal/mol. They later determined, however, that this bond dissociation energy is actually 25 kcal/mol (Ref. 19). Hence, their original estimate of the Cr(CO)_4^+ internal energy may be as much as 15 kcal/mol too low.
- (57) A.G. Joly and K.A. Nelson, J. Phys. Chem. **93**, 2876 (1989).
- (58) M. Lee and C.B. Harris, J. Am. Chem. Soc. **111**, 8963 (1989).
- (59) J.D. Simon and X. Xie, J. Phys. Chem. **90**, 6751 (1986).
- (60) J.D. Simon and X. Xie, J. Phys. Chem. **93**, 291 (1989).
- (61) J.D. Simon and X. Xie, J. Phys. Chem. **93**, 4401 (1989).
- (62) X. Xie and J.D. Simon, J. Am. Chem. Soc. **112**, 1130 (1990).
- (63) L. Wang, X. Zhu, and K.G. Spears, J. Am. Chem. Soc. **110**, 8695 (1988).
- (64) L. Wang, X. Zhu, and K.G. Spears, J. Phys. Chem. **93**, 2 (1989).

- (65) J.N. Moore, P.A. Hansen, and R.M. Hochstrasser, *J. Am. Chem. Soc.* **111**, 4563 (1989) and references therein.
- (66) S.-C. Yu, X. Xu, R. Lingle, Jr., and J.B. Hopkins, *J. Am. Chem. Soc.* **112**, 3668 (1990).
- (67) P.J. Hay, *J. Am. Chem. Soc.* **100**, 2411 (1978).
- (68) R.E. Winters and R.W. Kiser, *Inorg. Chem.* **4**, 157 (1965).
- (69) D.R. Bidinosti and N.S. McIntyre, *Can. J. Chem.* **45**, 641 (1967).
- (70) G.D. Michels, G.D. Flesch, and H.J. Svec, *Inorg. Chem.* **19**, 479 (1980).
- (71) F.I. Vilesov and B.L. Kurbatov, *Dokl. Akad. Nauk SSSR* **140**, 1364 (1961).
- (72) D.L. Lichtenberger and R.F. Fenske, *Inorg. Chem.* **15**, 2015 (1976).

TABLE I: Assignment of Photoions in the 248-nm MPI Mass Spectra of $\text{Cr}(\text{CO})_6/\text{CH}_3\text{OH}$ and $\text{Cr}(\text{CO})_6/\text{CD}_3\text{OD}$ Heteroclusters^a

S = CH_3OH^b	S = CD_3OD^b	Assignment
25, 26, 26.5, 27	25, 26, 26.5, 27	Cr^{2+}
28	28	CO^+
$33 + 32i$	$38 + 36i$	$\text{Sn}(\text{H/D})^+, n \geq 1$
50, 52, 53, 54	50, 52, 53, 54	Cr^+
68, 69	68, 70	$\text{CrO}^+, \text{CrO}(\text{H/D})^+$
80	80	$\text{Cr}(\text{CO})^+$
$84 + 32i$	$88 + 36i$	$\text{SnCr}^+, n \geq 1$
104, 136, 168	104, 140, 176	$\text{SnCr}_2^+, n = 0, 1, 2$
$112 + 32i$	$116 + 36i$	$\text{SnCr}(\text{CO})^+, n \geq 1$
$236 + 32i$	$252 + 36i$	$\text{SnCr}(\text{CO})_2^+, n \geq 4$
$240 + 32i$	$260 + 36i$	$\text{SnCr}(\text{CO})^+, n \geq 5$
$244 + 32i$	$268 + 36i$	$\text{SnCr}^+, n \geq 6$
$252 + 32i$	$256 + 36i^c$	$\text{SnCr}(\text{CO})_6^+, n \geq 1$
$256 + 32i$	--- d	$\text{SnCr}(\text{CO})_5^+, n \geq 2$
$312 + 32i$	--- e	$\text{SnCr}_2(\text{CO})_4^+, n \geq 3$
--- d	$460 + 36i$	$\text{SnCr}(\text{CO})_3^+, n \geq 8$

a) Reported m/z ratios are based on nominal atomic masses and do not include mass defects. Photoions corresponding to tungsten and molybdenum impurities were detected in minute amounts and are not tabulated here. The index, i , is a non-negative integer and obeys the relation: $i = n - 1$.

b) With the exception of those peaks assigned to Cr^+ and Cr^{2+} , reported m/z ratios of chromium-containing ions correspond to photoions which contain ^{52}Cr (rel. abund. 83.79%). Peaks corresponding to the less-abundant isotopes of many of the lighter photoions (e.g., SnCr_2^+) were observed in the mass spectra, but are not tabulated. These observations aided in further confirming our assignments.

c) Appears as trailing shoulder on the more-intense peak assigned to $(\text{CD}_3\text{OD})_n\text{Cr}(\text{CO})_2^+$.

d) Not observed.

e) Isobaric with $(\text{CD}_3\text{OD})_n\text{Cr}(\text{CO})_2^+$.

TABLE II: Thermochemical Data for Cr(CO)₆ and Coordinatively Unsaturated Chromium Carbonyl Species, Including Bond Dissociation Energies for Ions and Neutrals, First Ionization Potentials, and Ion Appearance Potentials

Species	Neutral BDE, kcal/mol	Ion A.P., ^a eV			Avg. Ion BDE, ^b kcal/mol	I.P., ^c kcal/mol
		Ref. 68	Ref. 69	Ref. 70		
(CO) ₅ Cr-CO	37 ± 5 ^d	8.15	8.48	8.42	25	185.2 ^e
(CO) ₄ Cr-CO	25 ± 5 ^d	9.5	8.95	9.85	19	173
(CO) ₃ Cr-CO	35 ± 15 ^f	10.7	9.84	10.45	28	167
(CO) ₂ Cr-CO	19 ^g	12.0	11.1	11.35	24	160
(CO)Cr-CO	19 ^{g,h}	13.1	11.94	12.51	39	165
Cr-CO	18 ^{g,h}	14.8	13.63	14.03	24 ⁱ	185
Cr	—	17.7 ^j	15.1	15.36	—	190 ^k

a) Appearance potentials reported in Refs. 68, 69, and 70 are precise to within ±0.3 eV, ±0.2 eV, and ±0.04 eV, respectively.

b) Estimates are based on average appearance potentials and are precise to within about ±15 kcal/mol.

c) Estimated from I.P. of Cr(CO)₆ and BDE's of ions and neutrals.

d) Ref. 19.

e) Ref. 71.

f) Ref. 34.

g) Average BDE's based on the difference between the sum of the first three BDE's listed (Refs. 19 and 34), and the heat of disruption (Ref. 54). Estimated precision is ±15 kcal/mol. This average value may be a poor estimate of the actual BDE's.

h) If the neutral BDE's scale as the ion BDE's, then BDE5 (for the neutral) may be considerably larger than, rather than equal to, BDE6.

i) This estimate is in good agreement with the calculated value of 21.5 kcal/mol for ⁴Σ Cr(CO)₂²⁺. See: Mavridis, A.; Harrison, J.F.; Allison, J. *J. Am. Chem. Soc.* 1969, 111, 2482.

j) This value was substantially greater than the two accompanying values and was not used for estimating an average A.P. for Cr⁺.

k) This value corresponds to ionization of ground-state Cr to the a ⁶D spin-orbit manifold of the ion. This is the lowest excited state of Cr⁺ with a 3d⁴4s configuration.

Figure 1. Experimental apparatus, shown schematically.
Photoionization laser and focusing optics are deleted for
clarity.

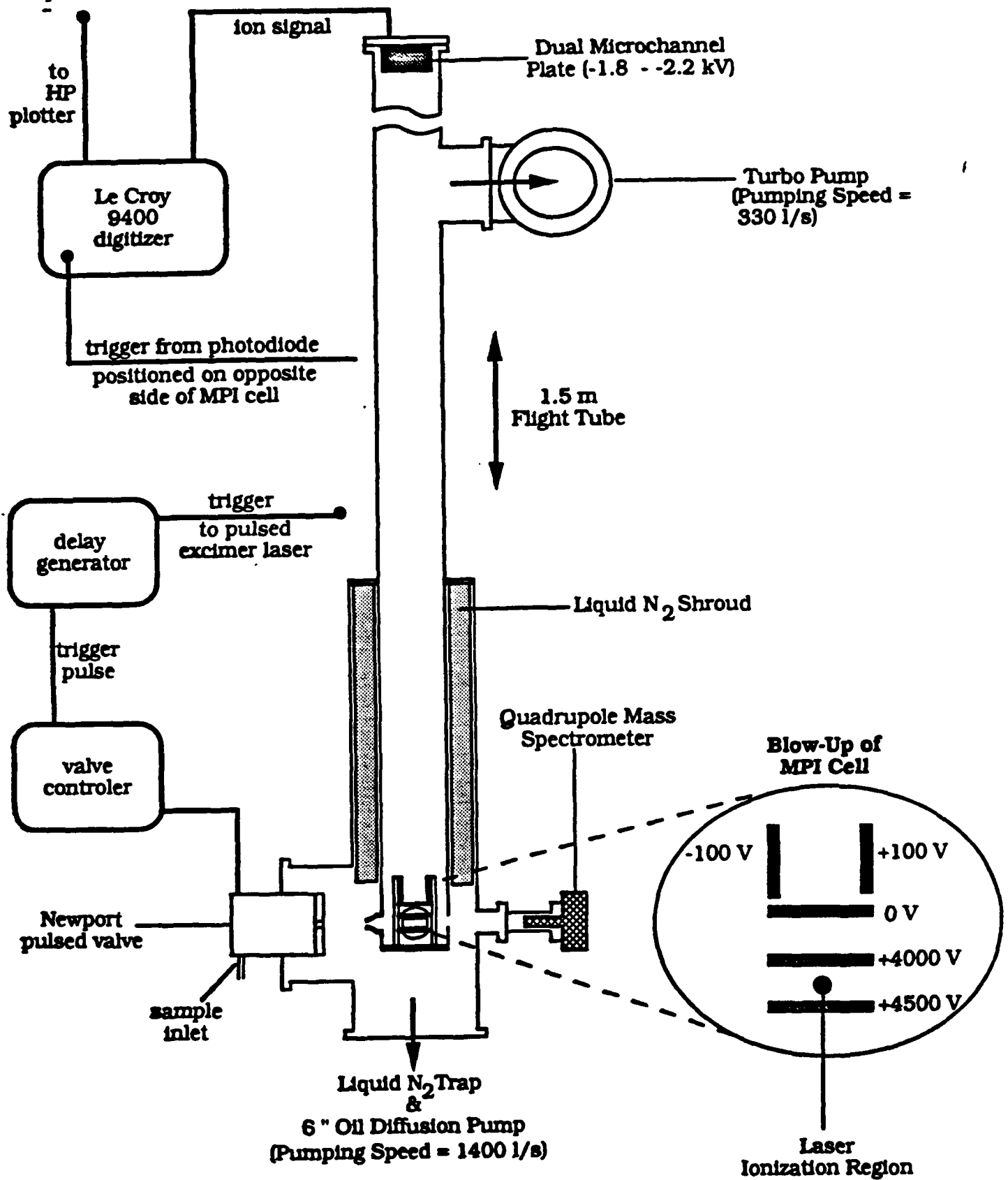


FIGURE 1, PEIFER + GARVEY, "UNUSUAL PHOTOFRAGMENTATION DRIVEN BY..."

Figure 2. Portion of the 248-nm MPI mass spectrum of $\text{Cr}(\text{CO})_6/\text{CH}_3\text{OH}$ heteroclusters. Integers above the peaks correspond to values of n , the number of CH_3OH molecules in an individual cluster ion. The sequence of binuclear cluster ions described in the text is not labeled, but first appears at $m/z = 312$ amu.

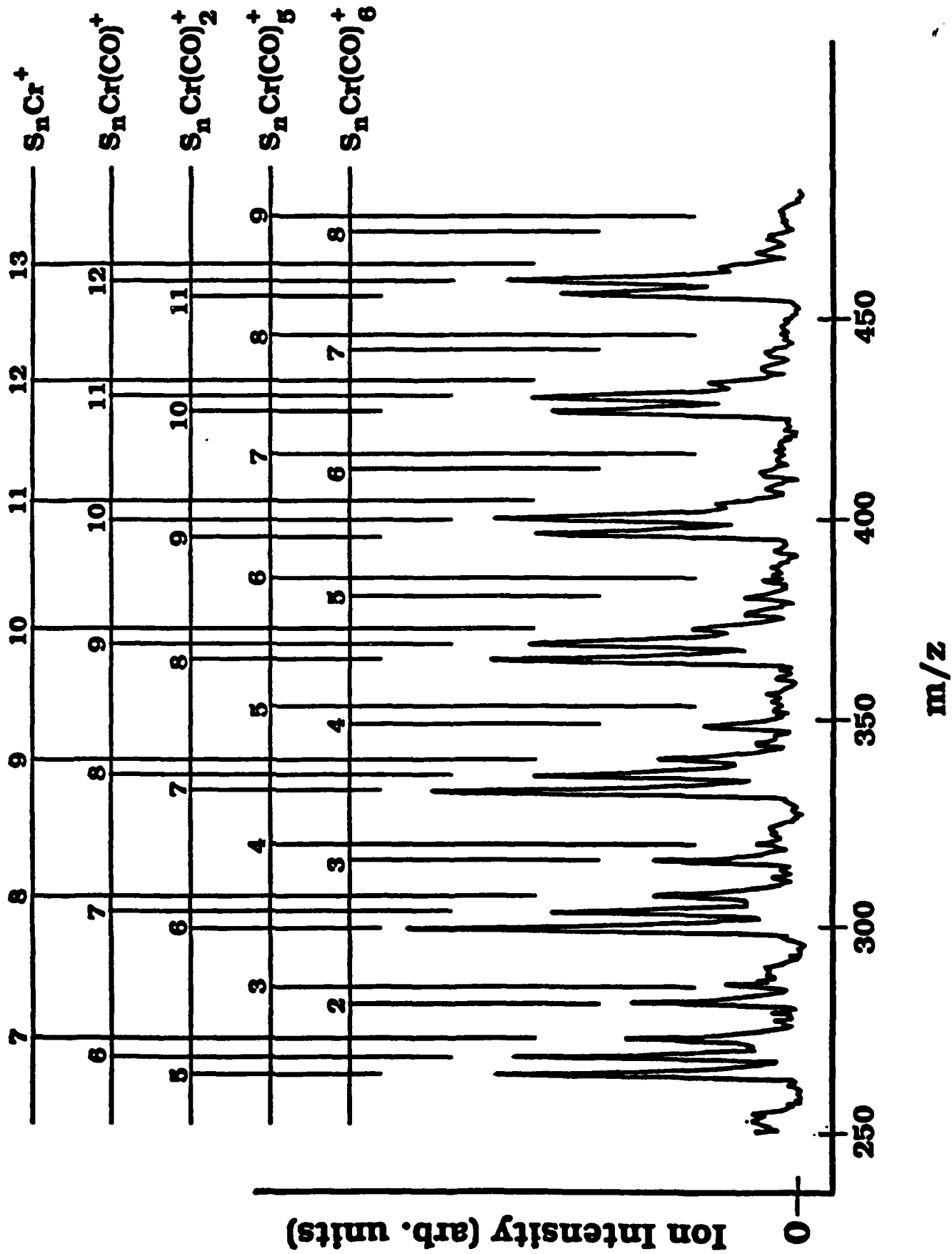


Figure 3. Portion of the 248-nm MPI mass spectrum of $\text{Cr(CO)}_8/\text{CD}_3\text{OD}$ heteroclusters. Peaks are labeled as in Figure 2. Peaks corresponding to $\text{S}_n\text{Cr(CO)}_8^+$ appear as trailing shoulders on the more intense peaks assigned to $\text{S}_n\text{Cr(CO)}_2^+$. Peaks attributable to $\text{S}_n\text{Cr(CO)}_5^+$, which would appear midway between $\text{S}_{n+3}\text{Cr(CO)}^+$ and $\text{S}_{n+4}\text{Cr}^+$, are conspicuously absent (see text). The peak which appears at $m/z = 460$ amu, 8 amu to the left of $\text{S}_{10}\text{Cr(CO)}_2^+$, is the first in a minor sequence of peaks attributed to $\text{S}_n\text{Cr(CO)}_3^+$. This sequence does *not* appear in the MPI mass spectrum of $\text{Cr(CO)}_8/\text{CH}_3\text{OH}$ heteroclusters.

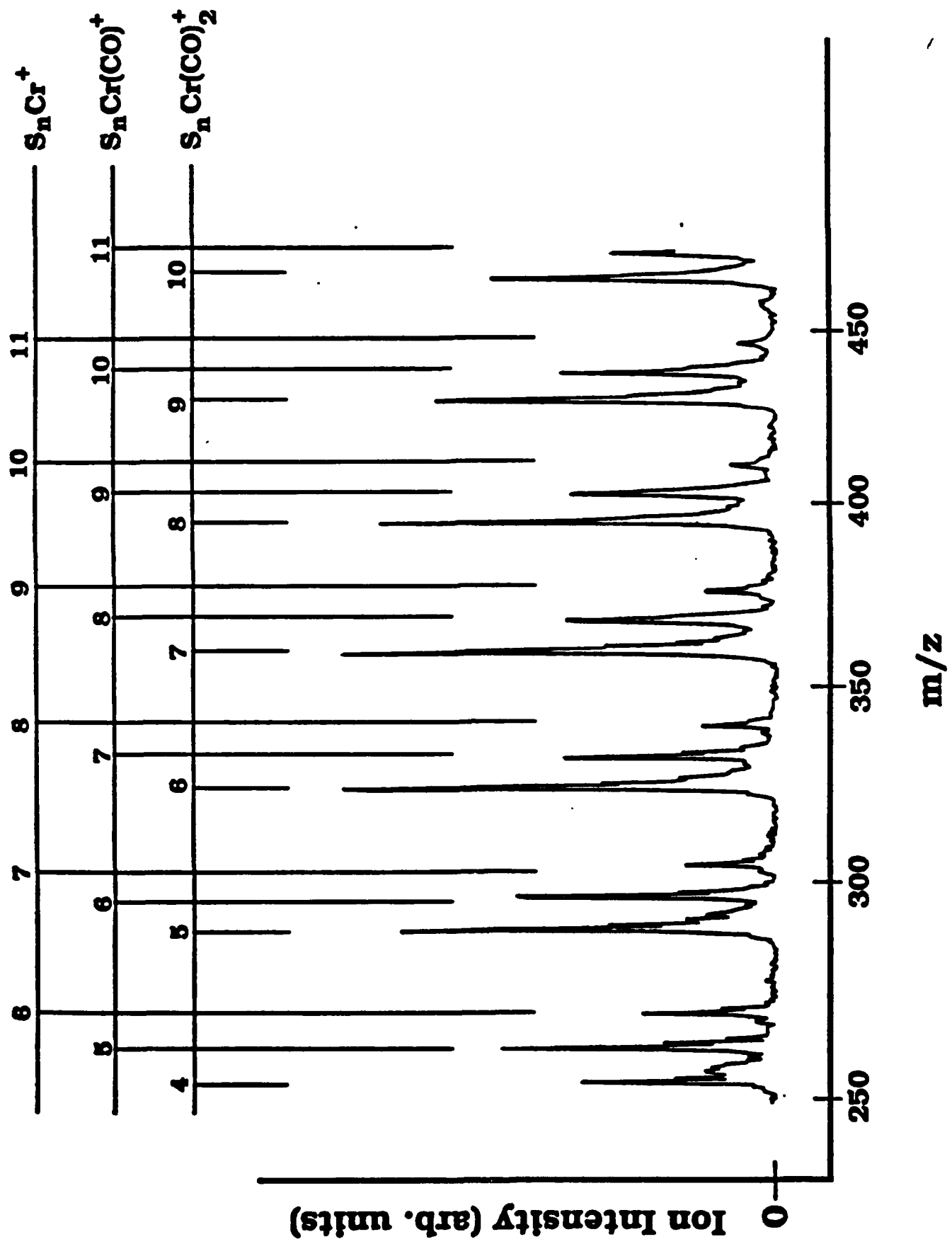


Figure 4. Energetics for sequential ligand loss in the neutral manifold. Spacings between species correspond to the respective bond dissociation energies. These values are taken from measured and estimated BDE's listed in Table II. The energy shown for chromium is for the ground electronic state (a^7S).

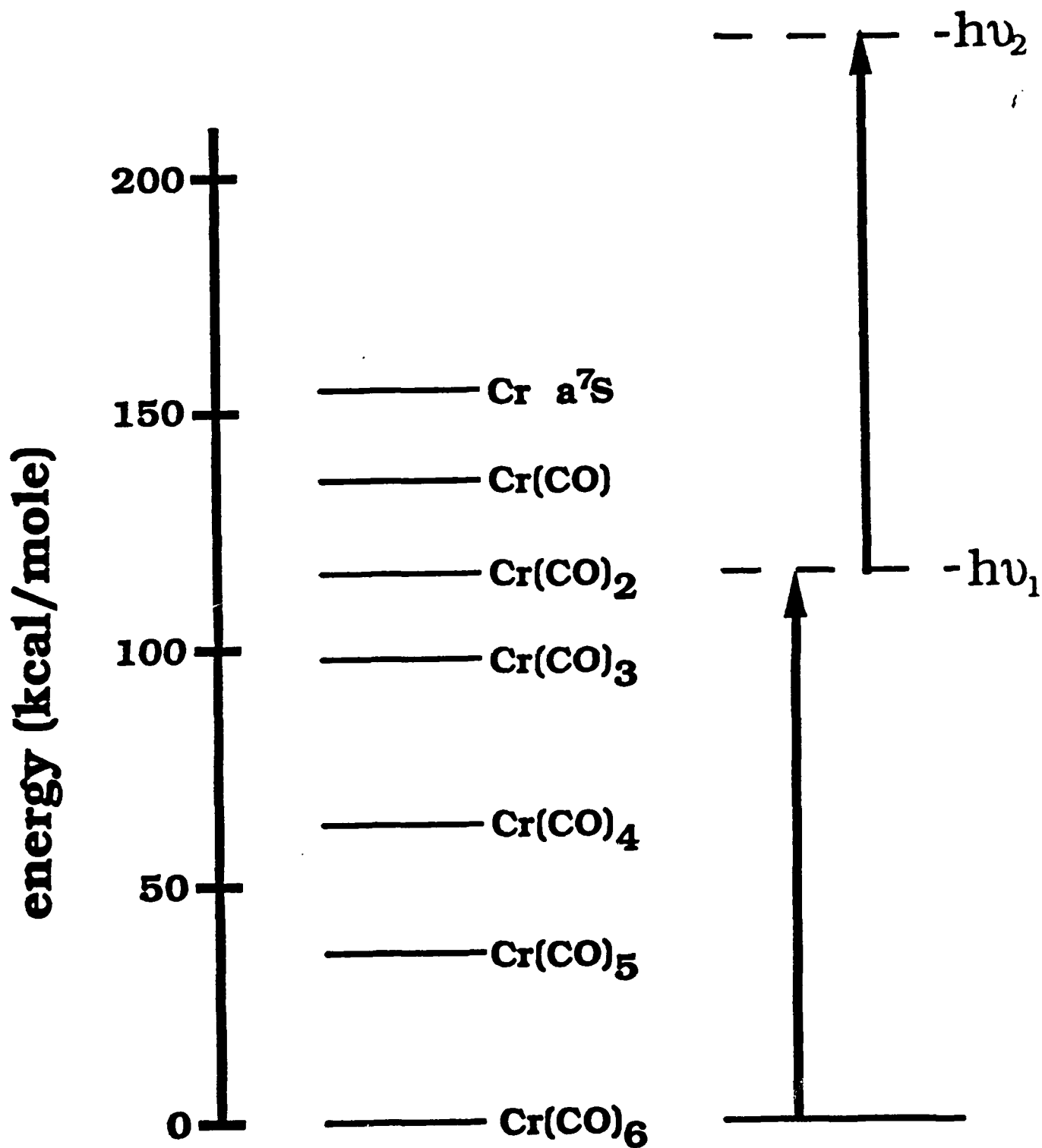


FIGURE 4. PETER & GARRY. "UNUSUAL PHOTOFRAGMENTATION DYNAMICS . . ."

Figure 5. General scheme describing the possible relationships between the various neutral and ionic species created through photodissociation and ionization.

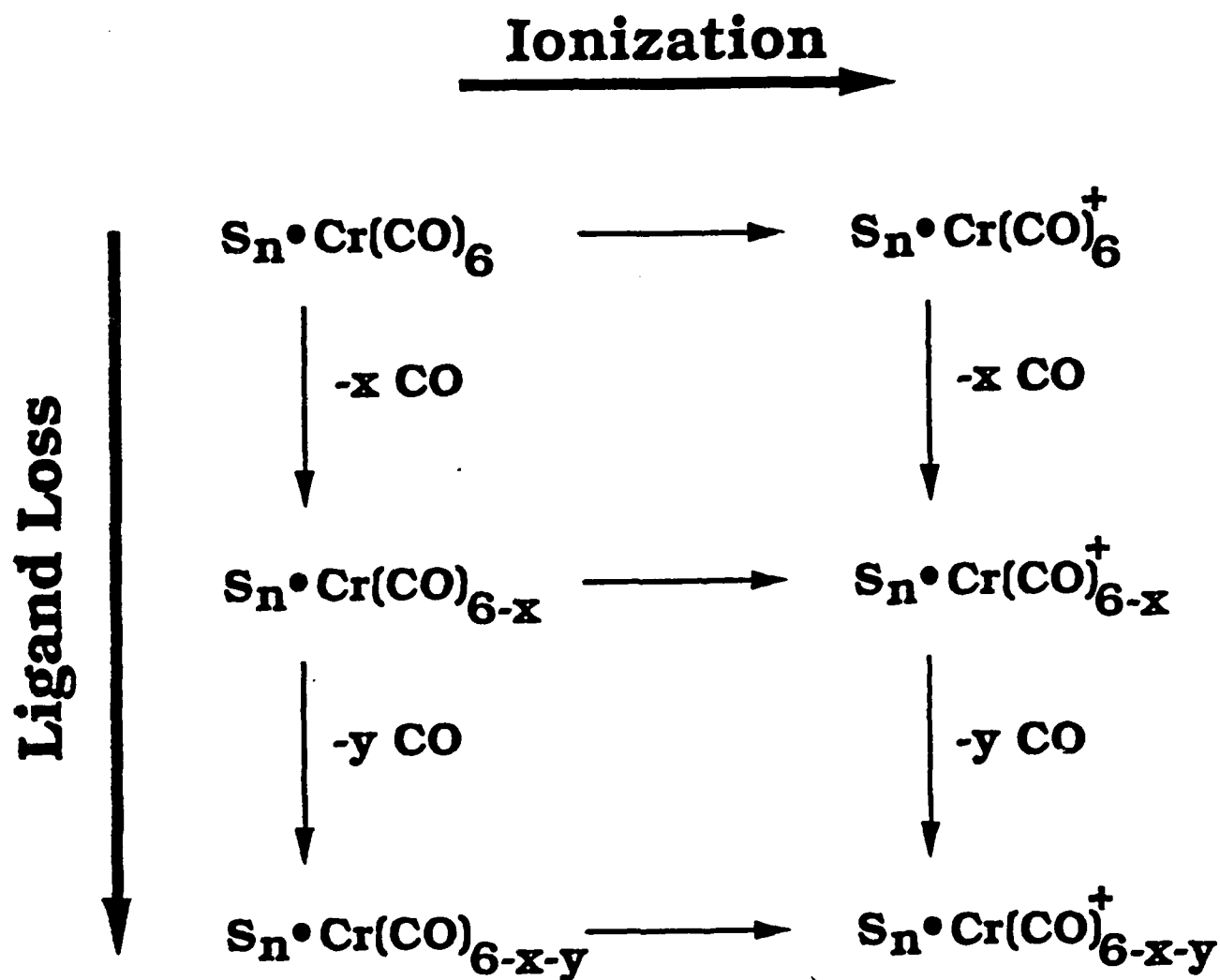


Figure 5, Petro: + GABLER, "UNUSUAL PHOTOFRAGMENTATION DYNAMICS..."

Figure 6. Proposed dynamical scheme describing photodissociation and multiphoton ionization of $\text{Cr(CO)}_5/\text{methanol}$ heteroclusters at 248 nm. Sequential photodissociation occurs in the neutral manifold down the length of the left-hand column, while non-resonant MPI takes place across the rows. The nascent photoions listed in the central column are internally excited and relax, either by predissociation or intracluster V-V energy transfer, to the ions listed in the right-hand column. The set, $\{k_3\}$, represents an ensemble of rate constants describing the relaxation of $S_n[\text{Cr(CO)}_4^*]^+$ to several smaller daughter ions. We have not attempted to explicitly describe the relaxation process(es) for $S_n[\text{Cr(CO)}_2^*]^+$, since we believe this to be the product of a minor channel. See text.

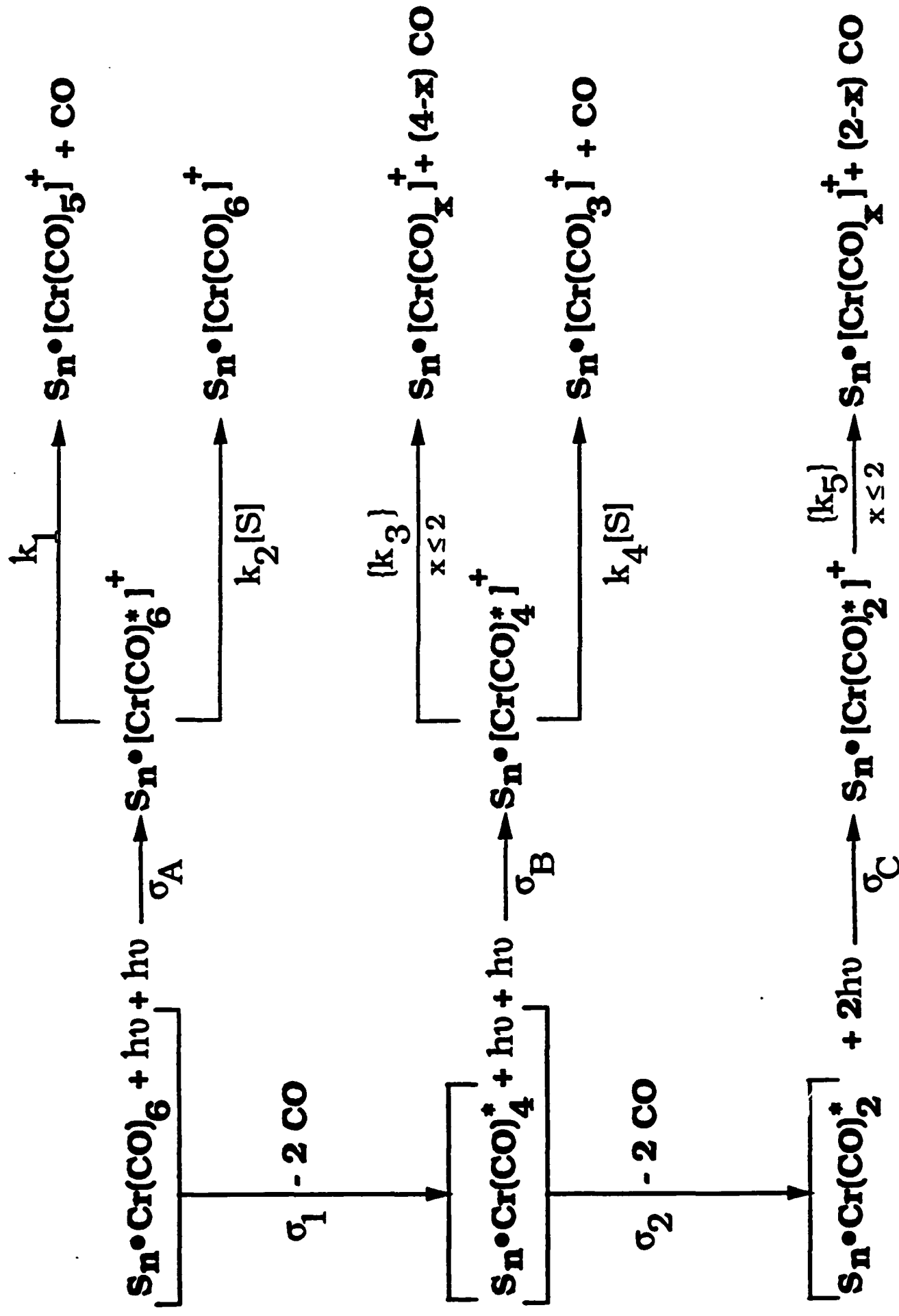


Figure 7. Energetics for sequential ligand loss in the ionic manifold. Spacings between species correspond to the respective bond dissociation energies. These values are taken from estimates listed in Table II. The energy shown for Cr^+ is for the lowest excited spin-orbit manifold (a^6D).

